

**Novel Techniques Studying the Polysaccharide  
Capsule of *Cryptococcus neoformans***

By

Camilla “Kip” A. Strother

A thesis submitted to Johns Hopkins University in conformity with the  
requirements for the degree of Master of Science

Baltimore, Maryland

April 2019

## Abstract

*Cryptococcus neoformans* is an environmental, fungal pathogen responsible for around 15% of AID-related deaths.<sup>1-3</sup> The primary virulence factor of *C. neoformans* is a polysaccharide (PS) capsule that inhibits phagocytosis by immune cells, interferes with complement, inhibits antibody production, and is necessary to cause disease.<sup>3-6</sup> The PS capsule is also the main drug and vaccine target. Even with current methods of isolation, the PS of *C. neoformans* has not been fully characterized. Throughout this work I will describe two novel methods of examining the PS of *C. neoformans*, sonication-induced cavitation to isolate the PS capsule, and neutron scattering to assess its structure. Cavitation, occurs when a bubble pops and the empty space is rapidly filled, induced by sonication was able to shave off the PS capsule. Released PS was detectable in the supernatant of sonicated samples, and antibody binding to the capsule still attached to the cell wall increased post-sonication. Neutron scattering was performed, for the first time, on the PS of *C. neoformans*, in collaboration with Dr. Susana Teixeira from the National Institute of Standards and Technology (NIST). There was no scattering from the PS in H<sub>2</sub>O and slight scattering from the sample in D<sub>2</sub>O. More work needs to be done to prepare samples used for neutron scattering before any conclusions can be made from the data. Novel techniques, such as those mentioned above, are important the continued characterization of the PS of *C. neoformans*, as well as for the discovery of more drug and vaccine targets.

Primary Reader: Dr. Arturo Casadevall

Secondary Reader: Dr. J. Marie Hardwick

## Acknowledgements <sup>1</sup>

The following people had a substantial influence on the work you are about to see:

Dr. Arturo Casadevall, Dr. Radamés J.B. Cordero, and Dr. Susana Teixeira.

I would also like to thank all the Casadevall Lab members, past and present. Special thanks to Quigly Dragotakes, Nina Grossman, Daniel Smith, and Raghav Vij.

I would like to thank Olive, as well as all of my family and friends who provided emotional support and guidance through the past two years. Without all of whom I would not be where I am today. Special shout out to: Dr. Cecilia Lenk, Dr. Paul Strother, Grace Strother, Anthony Burns, Alice Burns, and myself (for without whom literally none of this would have happened).

This work is dedicated to Kurtis P. Johnson.  
R.I.P.

---

<sup>1</sup> Acknowledgments were done alphabetically. Family acknowledgements were decided randomly.

## Table of Contents

<b>Acknowledgements</b>	<b>iii</b>
<b>List of Tables</b>	<b>v</b>
<b>List of Figures</b>	<b>vi</b>
<b>Introduction</b>	<b>1</b>
1.1 Thesis Statement	1
1.2 Background	1
1.3 Virulence Factors of <i>C. neoformans</i>	3
1.4 Composition of the PS Capsule	6
1.5 Structure of the PS Capsule	9
<b>Exploratory Method into the PS Capsule of <i>C. neoformans</i></b>	<b>11</b>
2.1 Sonic Cavitation	11
2.2 Small Angle Neutron Scattering	12
<b>Materials and Methods</b>	<b>14</b>
<b>Results</b>	<b>20</b>
4.1 Post-Sonication Images	20
4.2 Determining Culture Age	22
4.4 Effect of sonication as a function of time on <i>C. neoformans</i>	24
4.5 Determining Concentration of <i>C. neoformans</i>	27
4.6 Sonication of Isolated Exo-PS	30
4.7 Sonication and Antibody Binding	31
4.8 Small Angle Neutron Scattering of Exo-PS	33
<b>Discussion</b>	<b>35</b>
<b>Conclusion</b>	<b>41</b>
<b>Bibliography</b>	<b>43</b>
<b>CV</b>	<b>47</b>

## **List of Tables**

<b>Table 1. A comparison of different methods of <i>C. neoformans</i> PS isolation. ....</b>	<b>10</b>
<b>Table 2. Immunofluorescent images of un-sonicated and sonicated <i>C. neoformans</i> using different mAbs.....</b>	<b>32</b>

## List of Figures

Figure 1. Estimated yearly cases of cryptococcal meningitis in different regions of the world. ....	2
Figure 2. Two cross sections of isolated melanin from <i>C. neoformans</i> and close ups of the layers within melanin. ....	4
Figure 3. Cultures of melanized and non-melanized <i>C. neoformans</i> , H99.....	5
Figure 4. The six triads of <i>C. neoformans</i> GXM. ....	7
Figure 5. Total carbohydrate concentration of sonicated samples of <i>C. neoformans</i> . ....	10
Figure 6. Typical pattern of bubble cavitation behavior calculated from the Rayleigh-Plesset equation.....	11
Figure 7. The effect of sonication of non-melanized (left) and melanized (right) samples of <i>C. neoformans</i> , H99. ....	21
Figure 8. India ink slide of the reduction in <i>C. neoformans</i> PS capsule size post-sonication. ....	22
Figure 9. Total carbohydrate concentration as a function of sonicator setting of samples of <i>C. neoformans</i> . ....	22
Figure 10. <i>C. neoformans</i> survival after sonication as a function of sonicator setting.. ....	24
Figure 11. <i>C. neoformans</i> PS capsule diameter comparison between the waterbath sonicator and the horn sonicator. ....	26
Figure 12. Comparison of carbohydrate concentration in the supernatant of samples sonicated using either a waterbath (WB) or a horn sonicator (HS) using a phenol-sulfuric acid assay. ....	27
Figure 13. Total carbohydrate concentration post-sonication of supernatant samples. ....	28
Figure 14. GXM concentration of un-sonicated (0) and sonicated (7) samples of <i>C. neoformans</i> , H99 at different concentrations (cells/mL). ....	29
Figure 15. Effective diameter and polydispersity of sonicated 10kDa PS from <i>C. neoformans</i> .....	31
Figure 16. Neutron beam scattering readout of <i>C. neoformans</i> exo-PS, at different concentrations, in H <sub>2</sub> O on SANS. ....	33
Figure 17. Neutron beam scattering readout of <i>C. neoformans</i> exo-PS, at different concentrations D <sub>2</sub> O on SANS.....	34

# Introduction

## 1.1 Thesis Statement

New methods are needed to study the polysaccharide (PS) capsule of the fungal pathogen *Cryptococcus neoformans*. The PS capsule is the key to *C. neoformans* virulence, but due to its fragility, the PS capsule is difficult to characterize and the structure is unknown.<sup>3,5,7,8</sup> In this thesis I will describe two new methods, neutron beam scattering and sonication, for pursuing the structure of PS in the *C. neoformans* capsule and how these findings can advance efforts to characterize the PS capsule, why the use of findings from new techniques are of significance, and what are the next steps for continuation of this line of inquiry.

## 1.2 Background

*Cryptococcus neoformans* is an opportunistic fungal pathogen that causes cryptococcosis and can lead to cryptococcal meningitis.<sup>7</sup> It infects mainly immunocompromised individuals, particularly those living with HIV and AIDS.<sup>2,9</sup> *C. neoformans* has multiple virulence factors. The most important virulence factor is the polysaccharide (PS) capsule, which forms outside the cell wall of *C. neoformans*.<sup>10</sup> Another key virulence factor for *C. neoformans* is the ability to form a melanin layer in-between the cell membrane and cell wall.<sup>8,11</sup>

According to the Center for Disease Control and Prevention, CDC, around 220,000 people develop cryptococcal meningitis worldwide each year and it is responsible for around 15% of AIDS-related deaths.<sup>1,2</sup> The global burden of cryptococcal meningitis is primarily in sub-Saharan Africa where HIV and AIDS are prevalent (*Figure 1*). The CDC estimates that the number of deaths caused by cryptococcal meningitis is greater than that of tuberculosis in this population.<sup>1,2,12</sup>

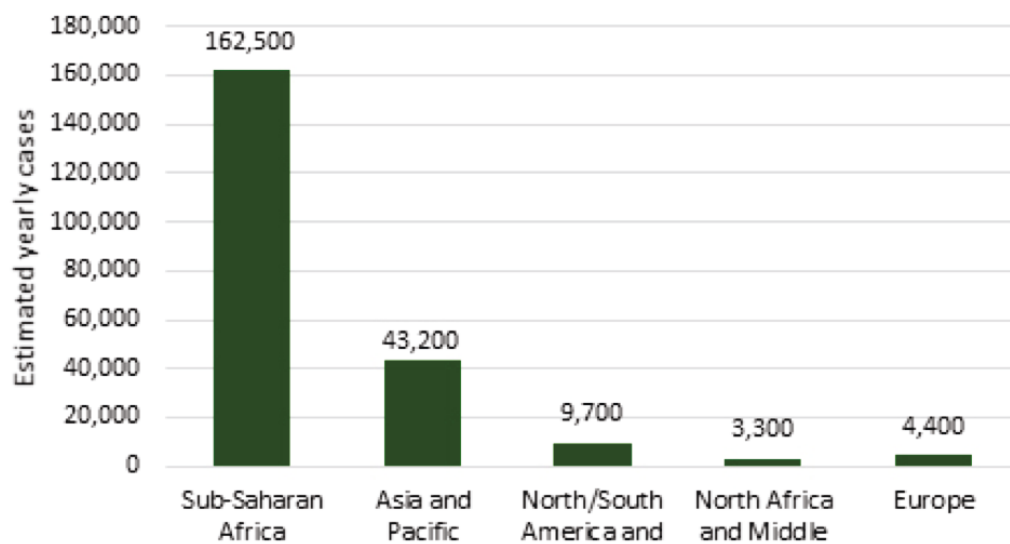


**Figure 1.** Estimated yearly cases of cryptococcal meningitis in different regions of the world. Figure obtained from the CDC, adapted from *R Rajasingham et al., Lancet Infectious Diseases 2017*.

This study primarily focuses on the PS capsule of *C. neoformans*, and briefly addresses whether melanized *C. neoformans* has increased protection from physical forces, cavitation in this case, compared to non-melanized. The research was conducted using several new methods, including sonication and neutron beam scattering, to provide new insights into structure of the PS capsule of *C. neoformans* and how changes in melanization may affect its virulence.



### 1.3 Virulence Factors of *C. neoformans*

The PS capsule is essential to causing disease in the host organism.<sup>7,8,11</sup> Without the PS capsule *C. neoformans* is avirulent.<sup>8</sup> The PS capsule enables *C. neoformans* to inhibit and evade the immune system through the following mechanisms.<sup>8,13,14</sup>

- Providing protection against host immune defenses;
- Inhibiting phagocytosis by macrophages;
- Inhibiting antibody production;
- Interfering with opsonic deposition of complement.

Because the PS capsule is the main virulence factor in *C. neoformans*; it is also the target for the development of therapeutic techniques and potential vaccines, as well as a medical biomarker for diagnosis.<sup>3</sup> The capsule structure is particularly difficult to study because of its highly branched structure, composition<sup>4</sup>, and fragility—all of which contribute to the difficulty of understanding the PS capsule in sufficient detail to develop an effective vaccine and therapeutic treatments. Most of the information about the capsular PS has been generated through the study of exopolysaccharide, which is released from *C. neoformans* in culture and can be removed and purified through several techniques.<sup>3</sup>

The ability to melanize is another critical virulence mechanism of *C. neoformans*.<sup>11,15,16</sup> The ability of *C. neoformans* to produce melanin can protect the pathogen from free-radical damage, oxidizing agents, and reduce the effects of amphotericin B, therefore increasing the pathogen's resistance to mammalian macrophages.<sup>15,17,18</sup> These are potential sources of damage to *C. neoformans* that can be found in either the environment or within a mammalian host.

Melanins are insoluble and complex biopolymers made up of phenolic and/or indolic compounds.<sup>15,19</sup> Using of catecholamines as substrates, for example, L-3,4-dihydroxyphenylalanine, *C. neoformans* synthesizes melanin layers between the cell

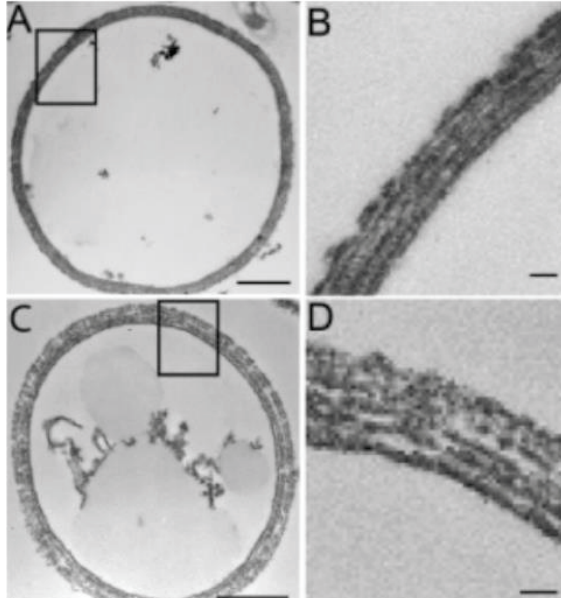


**Figure 2.** Two cross sections of isolated melanin from *C. neoformans* and close ups of the layers within melanin. There is no cell wall in this image. The age of the melanin increases from top to bottom. Scale bars are 1  $\mu$ m. This image is adapted from: Eisenman et. al. 2005. Microstructure of cell wall-associated melanin in the human pathogenic fungus *Cryptococcus neoformans*. Biochemistry 44(10), pp. 3683–3693.

membrane and cell wall. The layers of melanin vary in diameter from  $74 \pm 13$  nm to  $82 \pm 21$  nm (Figure 2). These size ranges correspond to the age of the fungal culture, grown in minimal media with L-3,4-dihydroxyphenylalanine at 30°C, the first being from a 1 week old culture and the latter 3 weeks.<sup>20</sup> This melanin layer, as seen in figure 2, is made up of 2-5 sub-layers that range in width from 50 and 75 nm with an average thickness of  $200 \pm 98$  nm.<sup>20</sup>

Melanins are classified into three major groups: eumelanins, pheomelanins, and allomelanins.<sup>21,22</sup> Eumelanin is the most common group and is responsible for brown and black pigments.<sup>23</sup> Pheomelanins are responsible for red pigment and allomelanins are from the plant kingdom.<sup>23,24</sup> The melanin in *C. neoformans* formed through the use of L-3,4-dihydroxyphenylalanine is classified as eumelanin. Figure 3 shows the visual

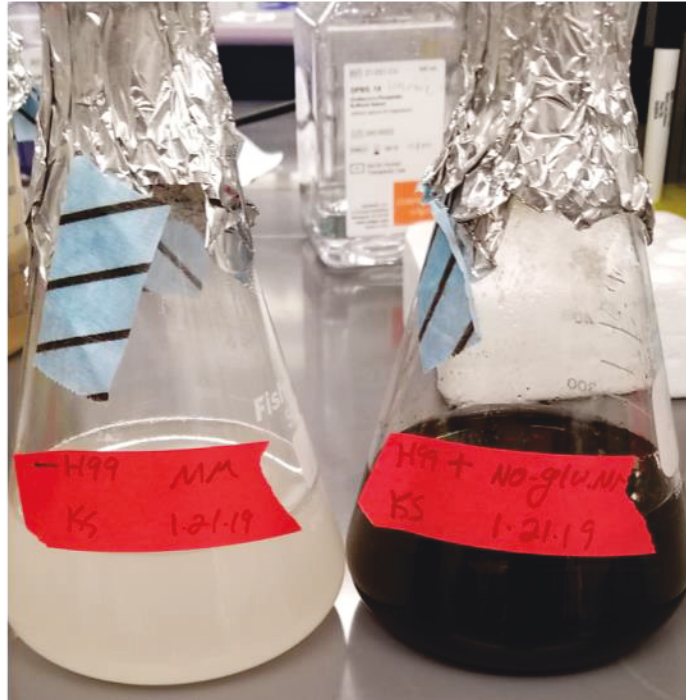


**Figure 3.** Cultures of melanized and non-melanized *C. neoformans*, H99. The culture on the left is non-melanized and the one on the right is melanized. Photo credit: Camilla A. Strother.

difference between *C. neoformans* cultures grown with and without L-3,4-dihydroxyphenylalanine. The response to produce this black eumelanin is catalyzed by a laccase called CNLAC1.<sup>25</sup> Despite the long history of melanin which was first being described as early as 1840 by Baron Jöns Jacob Berzelius, a Swedish scientist, a detailed structure of melanin compounds is not yet known though less complex structures are available.<sup>23,26</sup>

## 1.4 Composition of the PS Capsule

The PS capsule can grow several fold larger than the yeast cell diameter. Most of the PS capsule volume is comprised of water; the total mass and volume of the PS capsule is between 95% and 99% water.<sup>6</sup> This high water content makes the capsule prone to dehydration when studied using high resolution microscopy.<sup>6,27</sup> The PS capsule appears to be made up of layers, and is not uniform throughout its structure.<sup>28</sup> The PS component of the capsule is mainly glucuronoxylomannan (GXM) and glucuronoxylomannogalactan (GXM-Gal). GXM is the main PS in the capsule, making up 90-95% of polysaccharide components; GalXM comprises 5-8%.<sup>29</sup> Components of GXM are used as a targets for antibodies, which are used in detection and determining prognosis.<sup>30,31</sup> Mannoproteins have also been identified as capsular components, although their localization is generally at or near the cell wall. Other capsular proteins that have been identified include LHC1.<sup>3</sup>

There are two different genetically related subspecies of *C. neoformans*: *C. neoformans* var. *neoformans* and *C. neoformans* var. *gatti*. The two subspecies can be subdivided into four serological serotypes based on antibody reactivity to the GXM protein component. *C. neoformans* var. *neoformans* is made up of serotypes A, D, and A/D. Subgroup A includes H99, a common lab strain. Serotype A also makes up the majority of clinical isolates from cryptococcal infections in AIDS patient.<sup>32</sup> *C. neoformans* var. *gatti* is made up of serotypes B and C. For this project subgroup A, *C. neoformans* var. *neoformans*, strain H99 was used for all experiments.

The primary structure of GXM is made up of a linear (1→3)- $\alpha$ -D-mannopyranan bearing  $\beta$ -D-xylopyranosyl (Xylp),  $\beta$ -D-glucopyranosyluronic acid (Glc pA), and 6-O-acetyl substituents<sup>14,32</sup> (Figure 4) The location of the O-acetyl substituents is the major

factor that determines the antigen reactivity of the serotypes. This antigen type specificity is lost upon de-O-actylation of mannose residues.<sup>32,33</sup> The characterization of the primary structure of GXM was determined through the isolation of exo-PS. Exo-PS is PS that has been expelled from *C. neoformans*, and has been primarily used for GXM characterization due to ease of extraction.<sup>34,35</sup> Table 1, compares the different methods of both exo-PS and capsular PS extraction.

The structural components of GXM were determined using nuclear magnetic resonance also known as NMR.<sup>36</sup> NMR was also used to assign the proton chemical shifts of the de-O-acetylation of GXM. Using the anomeric protons of mannosyl residues as structure reporter groups (SRG) researchers were able to determine the distribution of the six mannosyl triads that are in GXM. This information was then used to chemotype *C. neoformans*.<sup>32</sup>

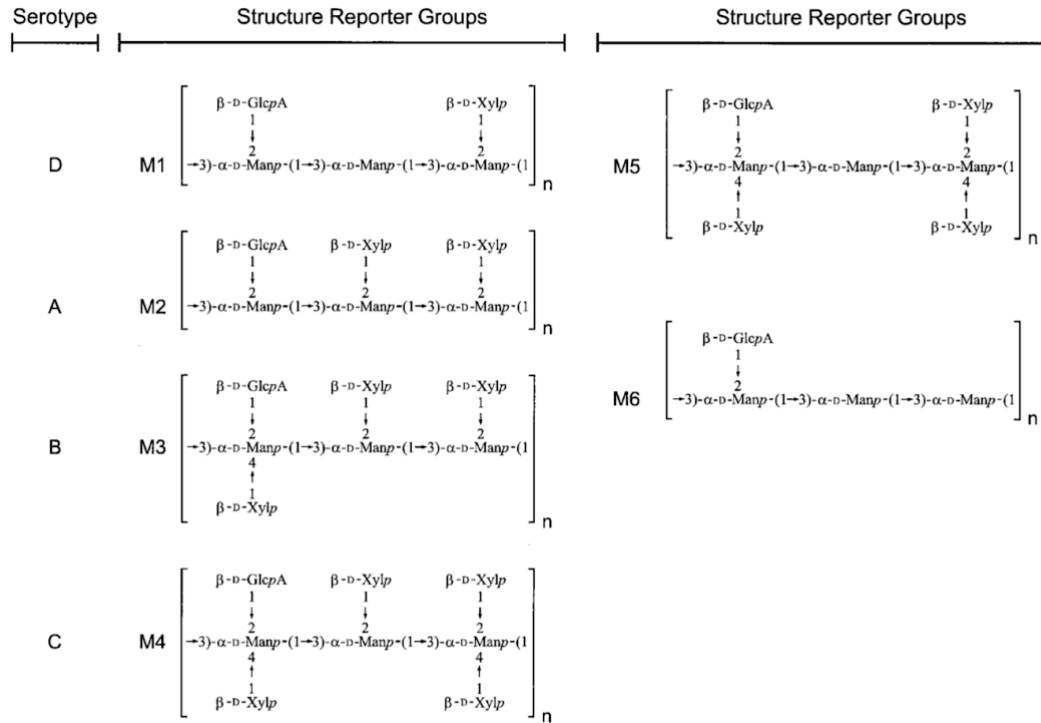


**Figure 4.** The six triads of *C. neoformans* GXM. Figure from Cherniak et al. 1998.

The primary structural components of GXM, derived from the use of NMR, were later confirmed and built upon through the use of mass spectrometry (MS). Using MS, the chemical components in the sample are ionized and sorted to determine mass-to-charge ratios.<sup>37</sup> The MS results confirmed the Man/GlcA ratio of GXM-derived oligosaccharides matched up with the 3:1 ratio that was hypothesized using NMR. This method also confirmed the GXM triad pattern shown in figure 4. The use of MS also provided new, important findings regarding the structure of the GXM molecule: the molecule can contain multiple triads of the six mannosyl triads available (*Figure 4*), the structure is highly heterogeneous, and can change depending on cell cycle and conditions.<sup>38</sup>

Two other methods that have been used to aid in the characterization of the PS capsule of *C. neoformans* are static light scattering (SLS) and dynamic light scattering (DLS). Both SLS and DLS measure how light is scattered through a sample. DLS works by changing the wavelength of the light. In SLS the concentration of the sample changes, and the wave length of light remains constant.<sup>39</sup> SLS and DLS are particularly advantageous for studying the PS capsule because they are non-destructive methods, and the sample remains in solution. Therefore, the data better reflects the PS in its native, hydrated state. SLS and DLS have been used to determine the average-molecular mass ( $M_w$ ); mean-square radius of gyration ( $R_g$ ); hydrodynamic radius ( $R_h$ ); and polydispersity.<sup>4</sup> These methods confirmed the previously suspected highly branched nature of the PS capsule.

## 1.5 Progress Toward Understanding the Structure of the PS Capsule

Despite the obstacle of capsular PS fragility there are methods to isolate it from the cell wall. However, these methods produce inconsistent results with one another (*Table 1*) This is due to the isolation methods themselves altering the PS of *C. neoformans*, which destroy the native composition and structure of the PS.

Two frequently used methods of capsular PS isolation involve the use of dimethyl sulfoxide (DMSO) and gamma radiation.<sup>40,41</sup> DMSO is quite a simple procedure where DMSO is added to *C. neoformans* cells, then the DMSO is dialyzed out leaving only the capsular PS. This method produces a high molecular weight PS (*Table 1*). This method is that it does not fully remove the PS capsule from *C. neoformans*, the inner most layer is still attached to the cell wall when observed with light microscopy. To completely remove the capsular PS different methods, like gamma irradiation, need to be performed.

Gamma irradiation is another commonly used method of capsular PS isolation.<sup>42</sup> This method is also quite simple and does fully remove the capsule from the cell wall.<sup>42</sup> There are drawbacks to this method, in particular the use of radiation which may not be a feasible tool for all research groups. The radiation also ionizes the -OH linages in the polysaccharide.<sup>28</sup> Both DMSO and gamma irradiation produce different molecular weights and sizes of capsular PS. Both of these techniques kill the cell; thus, some experiments that require living cells cannot be performed.

Method PS Isolation	Exo-PS Vs. Capsular PS	Molecular Size Rh(nm) Rg(nm) MW(10 <sup>6</sup> g/mol)	Polydispersity	Pros	Cons	Effect on Capsule
DMSO	Capsular	Rh: 907.9±14.1 Rg: 219.5±51.0 MW: 157.6±6.3	0.378±0.006	Simple procedure	Length of procedure	Increases the molecular weight of the sample
Gamma Radiation	Capsular	Rh: 178.7±2.1 Rg: 110.0±11.0 MW: 0.22±0.04	0.312±0.011	Quick, complete capsule removal	Radiation Ionizes the sample	Change the -OH linkages
Cetyltrimethylammonium Bromide Precipitation	Exopolysaccharide	Rh: 500.3±28.5 Rg: 44.3±7.3 MW: 0.87±0.07	0.459±0.010	High yield of polysaccharide	Length of procedure, can extract other stuff, killing of cells. Difficult to fully remove CTAB Structural changes through aggregation	Aggregates the capsule which may alter the structure
Supernatant Filtration	Exopolysaccharide	Rh: 262±18.4 Rg: 121.0±11.0 MW: 0.24±0.03	0.394±0.002	Cell free High volume of polysaccharide can be collected Can control the size collected	Length of procedure Risk of contamination Exopolysaccharide only	May not accurately represent capsule that is bound to the cell

**Table 1.** A comparison of different methods of *C. neoformans* PS isolation.



## Exploratory Methods into the Investigation of the PS Capsule of *C. neoformans*

### 2.1 Sonic Cavitation

The ultimate goal of this project is to understand how cavitation induced by sonication is altering the capsular PS of *C. neoformans* and how this information can be utilized to increase the knowledge about the native structure and composition of capsular

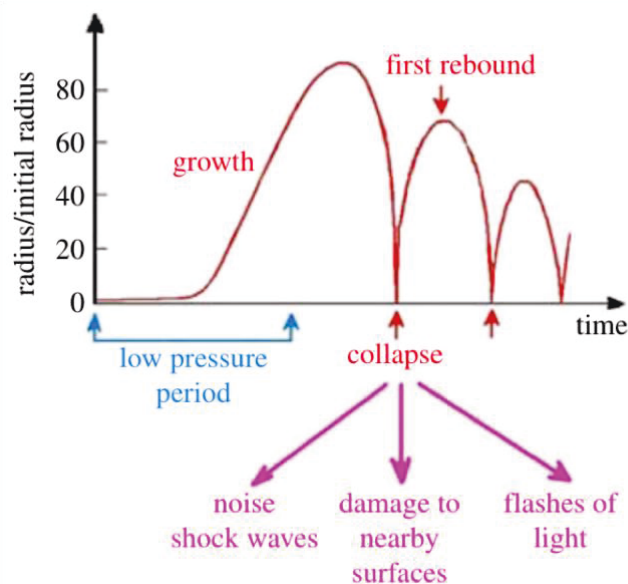


**Figure 6.** Typical pattern of bubble cavitation behavior calculated from the Rayleigh-Plesset equation. Figure from Brennen CE. 2015 Cavitation in medicine. Interface Focus.

PS. In liquids, sonic cavitation occurs when a bubble pops and the empty space is rapidly filled.<sup>43</sup> Figure 6, shows the typical behavior of bubble cavitation. This rapid change in pressure generates a shock wave that is powerful enough to pit the propellers on submarines.<sup>43,44</sup> Cavitation has been utilized in the medical field to do things such as emulsifying tissues for cataract surgery, or to control/alter DNA inside a cell.<sup>43</sup> Sonicators are used to induce cavitation within samples in the laboratory. Sonicators come in multiple forms with different power outputs. Water bath sonicators have a wide variety of uses and can be found both in homes and in laboratories. These machines are

essentially a bathtub where sound, emitting from all sides, induces cavitation within the water bath. The solid sample (or jewelry, or glasses) is placed in the water for a period of time to be lysed or cleaned. This method can take up to a few hours to fully work without the sample overheating. The downsides of this method are the low energy output; the time it takes to be fully effective; and that the cavitation cannot be focused. The probe or horn sonicator, which will be referred to later, uses the same basic idea except the sound waves are focused through a metal probe. The probe can be put into a liquid and induce cavitation. Horn sonicators reach higher energy outputs than the water bath sonicators, take less time to be effective, but also cause a rise in the temperature of the sample.

## **2.2 Small Angle Neutron Scattering**

To analyze the structure of exo-PS of *C. neoformans* we utilized the novel technique of neutron beam scattering. Ultra-small angle neutron scattering (USANS) and small angle neutron scattering (SANS) to characterize the PS of *C. neoformans* is being studied in collaboration with Dr. Susana Teixeira from the National Institute of Standards and Technology (NIST). These techniques used to study the structural information below 100nm.<sup>45,46</sup> Neutrons are non-ionizing, and thus, make excellent probes into matter, with tunable energies that cover a wide range of resolutions. They are also able to penetrate most materials non-destructively. The initial readout is a sigmoidal curve if signal is detectable, if there is no scattering it is a flat line. Any peaks or troughs in the curve correspond to possible structural components in the sample.<sup>45-47</sup> After the initial readout the data is reduced and fit to a model to continue characterization.

The ability to substitute deuterium, a stable isotope of hydrogen also called heavy water, with the labile hydrogen atoms within the sample allows for a better signal-to-noise ratio. This is because the deuterium isotope has a stronger coherent scattering (signal) and does not contribute to background noise as much as H. H/D exchange is performed with the use of D<sub>2</sub>O in the buffer which the sample is contained. Different contrasts (difference between the neutron scattering length density (SLD) of the molecule of interest in the sample, and the SLD of the buffer) are assessed by using a varying percent of D<sub>2</sub>O. This creates a difference in the scattering pattern where differences are highlighted, and certain components are matched out (zero-contrast). The  $q$  (scattering intensity) ranges for USANS are 0.00003-0.001 (inverse Angstrom) <sup>45</sup> and for SANS 0.001 to 0.4 (inverse Ang).<sup>48</sup> Data were reduced and analyzed with the NCNR, NIST Center for Neutron Research, macros for Igor Pro<sup>2, 47</sup>

---

<sup>2</sup> Access to USANS and NGB30SANS instruments was provided by the Center for High Resolution Neutron Scattering, a partnership between the National Institute of Standards and Technology and the National Science Foundation under Agreement No. DMR-1508249.

## Materials and Methods

### Cultures

A 6ml pre-culture of *C. neoformans* strain H99 was made in Sabouraud dextrose broth media. This pre-culture was incubated on a circulating rack for 24 h at 30°C. The cells were then washed three times with minimal media (15mM D-glucose, 10mM  $\text{MgSO}_4 \cdot 7 \text{H}_2\text{O}$ , 20.3  $\text{KH}_2\text{PO}_4$ , 3mM Glycine, 10mg/mL Thiamine). After washing, the cells were resuspended in 6mL of minimal media. Half (3mL) of the washed cells were inoculated into a flask with 500 mL of minimal media to grow the non-melanized *C. neoformans*. The other 3mL of pre-culture was inoculated into a flask containing 500mL minimal media containing 100mg of L-3,4-dihydroxyphenylalanine (L-dopa). These flasks were incubated in a 30°C shaker. The cultures were used at 3, 5, and 7 days.

### Sonication

A volume of 40mL, approximately  $1 \times 10^8$  cells/mL, of each 500mL culture were collected then washed with 1% PBS to remove all the spent minimal media. Cells were centrifuged at 15.6g for 7 minutes. Cells were counted and brought to a density of, or around,  $1 \times 10^8$  cell/mL in 1% PBS. From here, 2mL of the diluted cell suspension were put into glass tubes (volume and brand?). These tubes were then ultra-sonicated with the use of a horn sonicator (Fisher Scientific Sonic Dismembrator F550 W/ultrasonic Converter) for 30 seconds. Each sample was sonicated at one of the watts (RMS, root-mean-squared) levels (1-10) with tubes left unsonicated for control purposes. Watts (RMS) corresponds to a continues output of energy by taking several watt measurements

squaring each value, to determine the average, then finding the square root. Level 7 was the one that was primarily used. Post sonication cellular samples were used to do a “tadpoling” survival assay. Tadpoling<sup>49</sup> is an assay that determines whether the cells survived the treatment or not. It measures colony growth after a period of time. Treated samples were centrifuged at 13.3 g for 12 minutes. The supernatant was collected, and the pellet was used for microscopy.

### Survival Analysis

A tadpoling assay was used to evaluate yeast survival after sonication. This assay was adapted from Welch and Koshland, 2013<sup>49</sup>. A volume of 300  $\mu$ L of each sample were placed in the first row of a 96-well plate in triplicate. 200  $\mu$ L of Sabouraud dextrose broth was placed in the rest of the rows. The samples were serially diluted (1:3) down the rows. Sterile water was used as a control. Plates were placed in a 30°C incubator for 24-hours. Plates were imaged using and immunocapture 6.3.

Using ImageJ, the mean grey area was calculated from rows B-H on the 96-well plate was determine. This number corresponds to the number of colonies in the space with a lower number corresponding to fewer colonies. An average level of background was subtracted from the values attained to account for the color of the media in the wells. These data points were then normalized with the first 1:3 dilution of the control being 100%. From here survival curves were generated for non-melanized and melanized cultures at culture ages of 3, 5, and 7 days.

## Light microscopy

Light microscopy images of *C. neoformans* pre and post sonication were taken by mixing 3uL of the centrifuged cell pellet with 6uL of India Ink. Images were taken using (Microscope).

## Dynamic Light Scattering (DLS)

Polydispersity and effective diameter of samples was measured using a Zeta Potential Analyzer (Brookhaven Instruments Corporation). The methods used were described in Frases et al., 2009<sup>4,10</sup>.

## GXM Capture ELISA <sup>50</sup>

This method was adapted from Casadevall et al., 1992 <sup>50</sup>. Using a 96-well microtiter plate the wells were coated with 50ul/well of a 1-10ug/mL solution of anti-CNPS/GXM mAB, known as 2D10. This solution was prepared using 1X PBS. Plates were incubated for 1 hour at 37°C. Plates were blocked with a 1% BSA solution (prepared in 1X PBS) 200 µl/well, overnight at 4°C. A 10ug/mL GXM standard was used for the standard curve. 75ul of sample or standard was added to the first well in each column, then 25ul was serially diluted into 50ul of 1X PBS horizontally across the plate. The plate was then incubated at 37°C for one hour. Plates were then washed 3 times with 0.1% TWEEN-20 in TBS. Next 50 µl/well of an anti-CNPS/GXM mAB of a different isotype than the initial one, 18B7, was diluted to a concentration of 2 µl/mL in blocking solution and added to the wells. The plate was then incubated at 37°C for one hour or at

4°C overnight. Plate was then washed 3 times with the same solution previously mentioned.

Then 50µl/well of a 1:1000 dilution of alkaline phosphatase labeled anti-Fc Ab that would recognize the mAb 18B7 (IgG1), was added, dilutions were again made in blocking solution. Plate was then incubated at 37°C for one hour or at 4°C overnight. Plate was then washed 5 times with the above solution. 50 µl/well of 1 mg/ml alkaline phosphatase substrate (p-nitrophenyl phosphate) in substrate buffer were then added. Plates were given time at room temperature to develop then read at A<sub>405</sub>. The amount of GXM in each sample was determined by plotting the standard along a logarithmic x-axis. The linear portion of that s-curve was then fitted with a linear regression line. Only samples with absorbances in this linear range were used to calculate the total GXM in the sample. This was done by plugging the absorbance into the equation given by the linear regression, multiplying by the dilution of the sample, then multiplying by the volume the sample was initially resuspended in.

#### Phenol-Sulfuric Acid Assay <sup>51</sup>

This assay was developed from Maskuko et al., 2005. To start 100µl of 1M mannose was 1:2 serially diluted into 50µl of sterile water in the first three columns of a 96-well plate. 50µl of each sample was put into three wells undiluted. A volume of 50µl of sterile water was placed in three wells to determine background. 150µl of concentrated sulfuric acid was placed in each well. 30µl of a 5% phenol solution was pipetted into each well. The 96-well plate was then incubated at 37°C for about 10 minutes. Plate was read at read at A<sub>490</sub>.

### Immunofluorescence Staining

Samples were blocked in blocking buffer (1% bovine serum albumin (BSA) in 1XPBS) for 30 minutes at room temperature. After, samples were washed once with blocking buffer. UVTex 2B (5 $\mu$ /mL), and Nile Red (5 $\mu$ /mL) were added with the primary mAbs (18B7, 2D10, 12A1) to blocking buffer. Primary mAbs were brought to a concentration of 10 $\mu$ g/mL. Samples were set to incubate on a shaker at 30°C for 30 minutes. Post incubation samples were washed 3 times with blocking buffer. Post-washing FITC-secondary antibody conjugated at 2 $\mu$ g/mL was added to blocking buffer then added to the samples. For 18B7 goat anti-mouse IgG was used. For 2D10, and 12A1 goat anti-mouse IgM was used as the secondary antibody. Samples were set to incubate on a shaker at 30°C for 30 minutes. Post incubation samples were washed 3 times with blocking buffer. Slides were prepared using 3 $\mu$ L of India ink combined with 6 $\mu$ L of sample.

### Exo-PS Prep for Neutron Scattering

A 3mL pre-culture of *C. neoformans* strain H99 was made in Sabouraud dextrose broth (SAB) media. This pre-culture was incubated on a circulating rack for 24 h at 30 °C. The cells were then pelleted and washed with minimal media to remove the spent media. The pellet was then inoculated into a 1L culture of minimal media to induce capsule growth. The flask was placed on a shaker at 30 °C for 7 days. After the 7 days the culture was spun down to pellet the cells. The supernatant was then removed and run through a 0.22 $\mu$ m vacuum filter to remove any lingering cells. This cell-free supernatant



was then run through an Amicon with a series of different sized membrane (100kDa, 30kDa, 10kDa, and 1kDa). The gel collected from the 10kDa membrane was split into two falcon tubes and either D<sub>2</sub>O or H<sub>2</sub>O was added.

## Results

The ultimate goal of this project was to determine what effect cavitation induced by sonication was having on the structural and compositional components of the capsular PS of *C. neoformans*. The following experiments were designed to test the effects of time in culture, survival, and cell density on the samples of *C. neoformans* used for cavitation experiments. Once each condition was optimized, the resulting experimental were applied thereafter to address the questions: what was the fate of the capsule structure post-sonication, and where there any compositional changes in the PS post-sonication?

### 4.1 Post-Sonication Images

To determine the effect of sonication on overall structure of the PS I imaged *C. neoformans* pre and post-sonication using light microscopy and observations of pellets post-centrifugation.

In figure 7, approximately  $1 \times 10^8$  cells/mL were sonicated then centrifuged, and the volume of the pellets were observed by eye to determine that the post-sonication samples had a smaller sample volume. This was the case for both melanized and non-melanized samples.

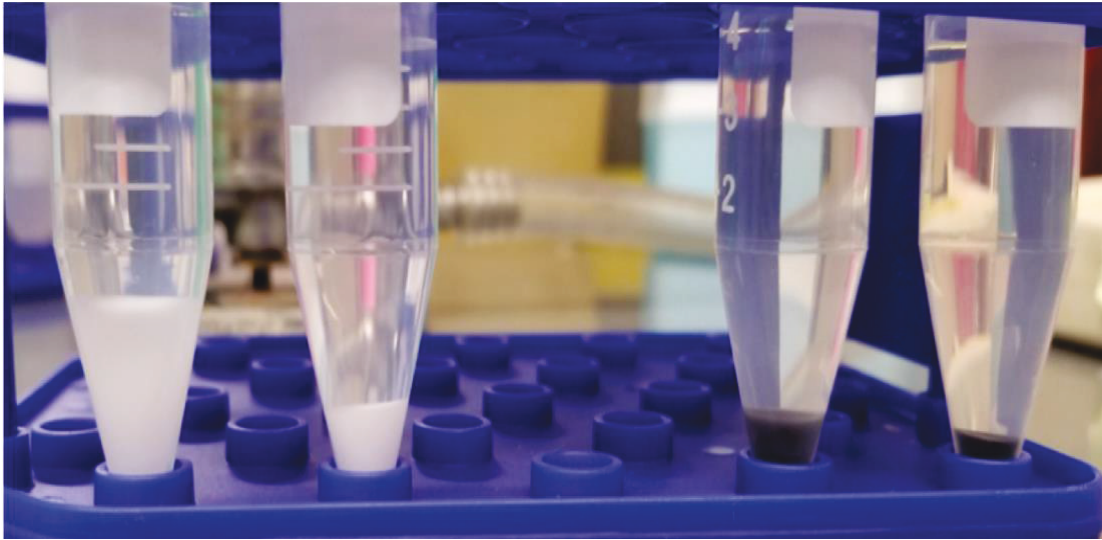


**Figure 7.** The effect of sonication of non-melanized (left) and melanized (right) samples of *C. neoformans*, H99. Un-sonicated samples are the ones in the left for each pair. Sonicated samples are on the right for each pair. Photo credit: Camilla A. Strother

Light microscopy of sonicated and un-sonicated non-melanized *C. neoformans* showed a decrease in capsule radii post-sonication (*Figure 8*). Images were taken using India ink, in order to give contrast to the PS capsule. Figure 8 compares sonicated and un-sonicated non-melanized *C. neoformans*. These observations lead me to further explore the effects of sonication on capsule structure and composition. These images suggested that the PS capsule was being removed through sonication. This led me to look into what was happening to the PS and the cell post-sonication.

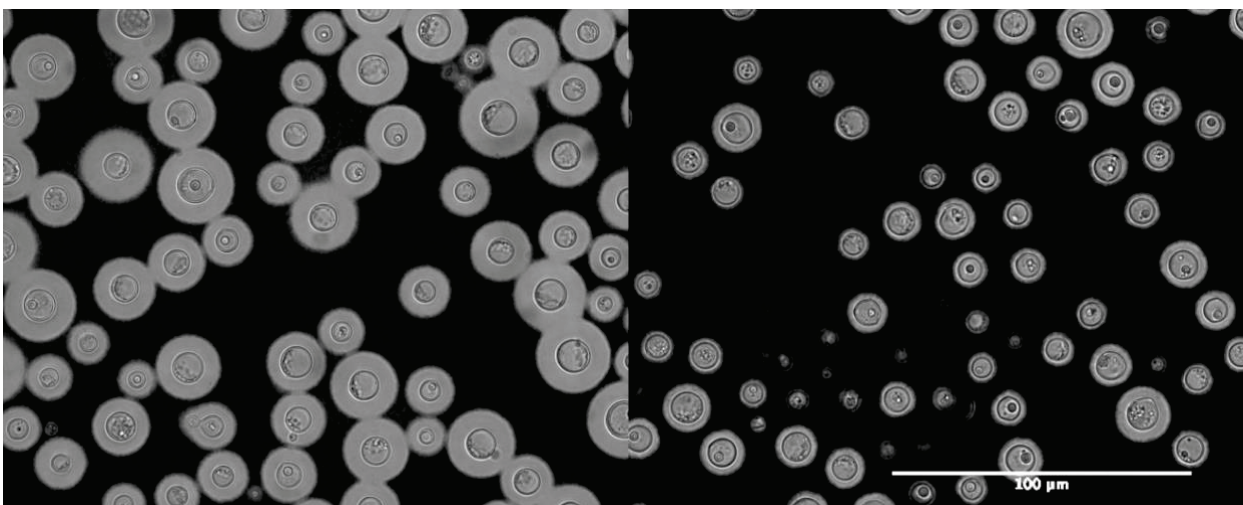


**Figure 8.** India ink slide of the reduction in *C. neoformans* PS capsule size post-sonication. Non-melanized *C. neoformans*, H99, at 40X using an India ink stain. The red arrows indicate the PS capsule. The sample on the left is un-sonicated. The sample on the right is sonicated. There is a reduction in capsule size post sonication.

## 4.2 Determining Culture Age

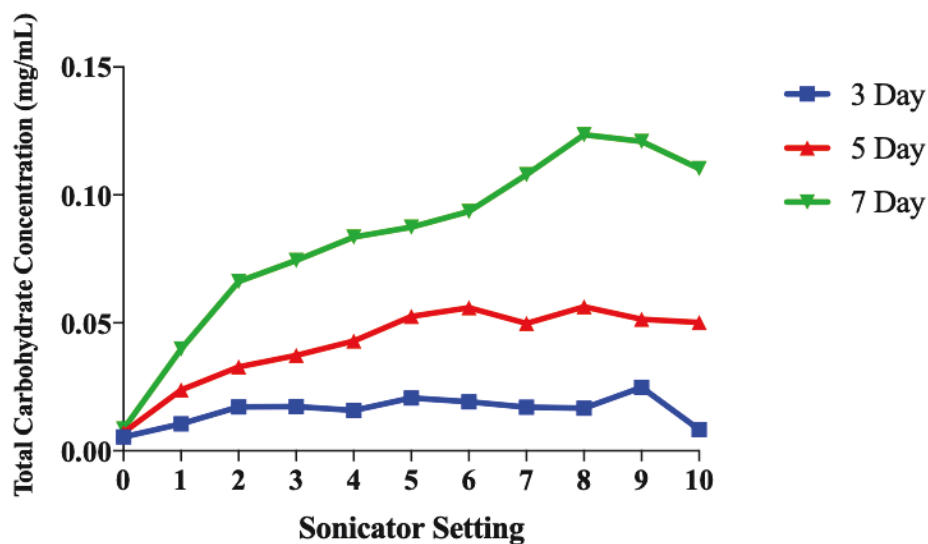


**Figure 9.** Total carbohydrate concentration as a function of sonicator setting of samples of *C. neoformans*. This was done in order to look at the optimal setting and age for the culture. Phenol-sulfuric acid assays were performed to obtain this data.

The PS capsule of *C. neoformans* is reported to undergo biophysical and chemical changes with age.<sup>13</sup> To determine what culture age is optimal for further experiments, samples of non-melanized *C. neoformans*, H99, were sonicated for 30 seconds at each

power level (1-10) on days 3, 5, and 7 (Figure 9). Non-melanized *C. neoformans* was used because it produces a larger capsule than melanized *C. neoformans*. Based on phenol-sulfuric acid assay, to detect all total carbohydrate concentration in a sample (data in figure 9), I determined that the day 7 culture had the highest overall levels of detectable carbohydrate. PS capsules are composed of polymeric carbohydrates, and the carbohydrate content was quantified using a phenol-sulfuric acid assay. Figure 9 also shows that a setting of 8, on a Fisher Scientific Sonic Dismembrator F550 W/ultrasonic Convertor, produced the highest level of carbohydrate which corresponds to the level of *C. neoformans* PS in the sample. Despite these results, a culture age of 5 days was chosen to continue the experiments. A 5-day old culture is more representative of the vegetative state of the *C. neoformans* capsule, as the composition changes with age.

### **4.3 Effect of sonication on *C. neoformans* survival**

The survival of *C. neoformans* post-sonication was determined at a range of sonication levels to optimize the protocol. This was done by sonicating at levels 1-10 on the sonicator, with 1 having the lowest watts (RMS) power output and 10 the highest. All samples were sonicated for 30 seconds on 5-day-old cultures. There was an increase in the amount of capsule that was released from the sonicated cells as the power was increased. However, more cells were killed at the higher setting, as determined through tadpole assays. Tadpoling assays measure cell survival by measuring growth in a 96-well plate. The sample is put into the first row of the plate then diluted down the columns. Survival itself is determined by measuring the mean grey pixel value of each well using ImageJ. A higher mean grey value means more growth thus a higher survival rate.

Through tadpoling assays I determined that a setting level of 7 (approximately 20 watts (RMS)) was the best level to get noticeable levels of capsule shaving with good cell survival (*Figures 9 and 10*). Figure 10 is made up of graphs from the tadpoling assay analysis. Here, a steeper curve indicates lower survival rate. Based on these results as well as those from the culture age experiments, I decided to continue with a sonicator setting of 7 and a 5-day-old cultures as they appeared to be the best conditions for further experiments due to a moderate level of detectable PS post-sonication as well as cell survival.

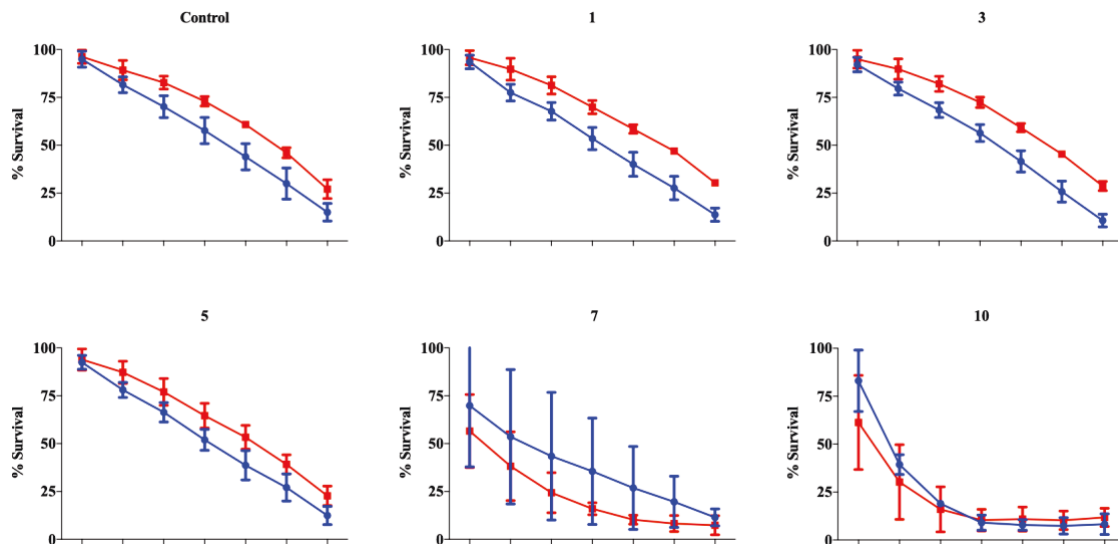


**Figure 10.** *C. neoformans* survival after sonication as a function of sonicator setting. The % survival (y-axis) of sonicated *C. neoformans*, H99, both melanized (blue) and non-melanized (red). These cells were all from 5-day old cultures. The x-axis is a 1:3 dilution series. There is overall good survival from *C. neoformans* post sonication until the sonicator is changed to 7. From here there is a drop off in survival. Based on these results and the results of phenol-sulfuric acid assay date a level of 7 for the sonicator was chosen to continue with experiments. % Survival was determined using tadpoling assays then the mean grey values were determined using ImageJ.

#### 4.4 Effect of sonication as a function of time on *C. neoformans*

To further optimize PS isolation procedures, different sonication methods and times were tested. A comparison was made between water bath sonication (Branson,

Branson® CPXH Ultrasonic Bath, Model 2800) and the use of the horn sonicator (Fisher Scientific Sonic Dismembrator F550 W/ultrasonic Converter). The cells in the water bath were kept in for two hours on the high (40kHz) setting. For the horn sonicator (50-60kHz) *C. neoformans* was sonicated for 30 seconds at power setting 7 (approximately 17 Watts (RMS)<sup>3</sup>). For the horn sonicator the output is given in Watts (RMS)<sup>4</sup>. The samples did rise in temperature post-sonication (on average by 16°C<sup>5</sup>, but this did not reduce survival (no ice bath was used for the survival assay samples), or the amount of capsular PS released.<sup>6</sup> This is based on an experiment where an ice bath was used to keep the sample from overheating. Capsule size measurement data (*Figure 11*) indicate that both methods are effective for reducing the diameter of the PS capsule of *C. neoformans*. However, based on the phenol-sulfuric acid assay results (*Figure 12*) the water bath method is not as effective in removing the capsule of *C. neoformans*. Therefore, I continued all subsequent experiments with the horn sonicator.

---

<sup>3</sup> N=21 readings of the sonicator during experiments.

<sup>4</sup> More information on Watts (RMS) can be found in “Materials and Methods” under Sonication.

<sup>5</sup> N=14 before and after sonication temperature readings.

<sup>6</sup> Data on this is not shown.

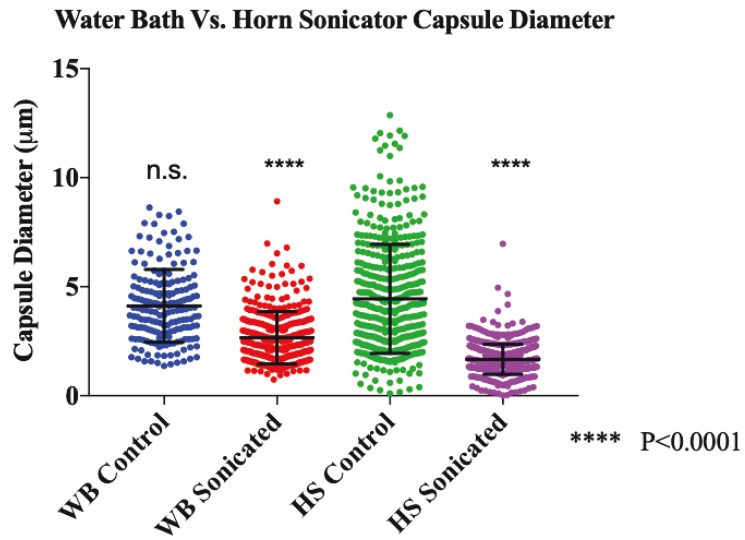


**Figure 11.** *C. neoformans* PS capsule diameter comparison between the water bath sonicator and the horn sonicator. Measurements were taken from microscopy images and run through a capsule measurement program. There is a significant difference between the sonicated (treated) samples for both the horn sonicator and the water bath. There was no significant difference between either of the untreated samples. Significance was determined using multiple comparisons in a one-way ANOVA.



### Water Bath vs. Horn Sonicator Carbohydrate Concentration

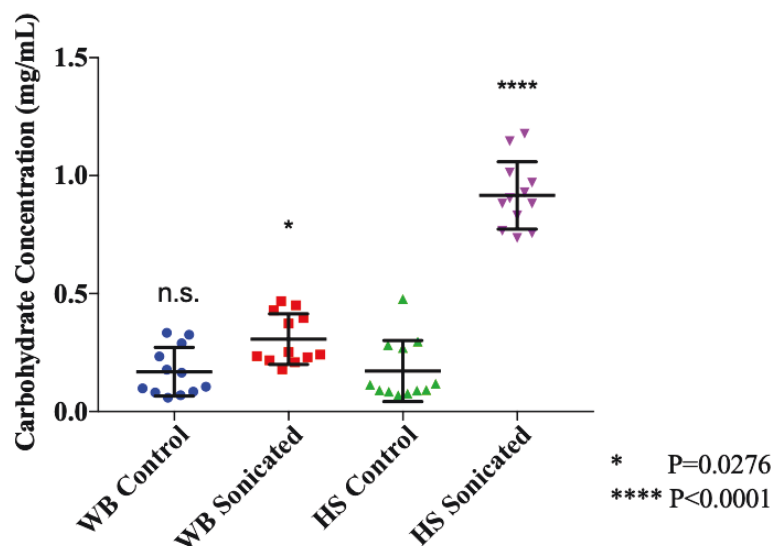


**Figure 12.** Comparison of carbohydrate concentration in the supernatant of samples sonicated using either a water bath (WB) or a horn sonicator (HS) using a phenol-sulfuric acid assay. Based on a one-way ANOVA using multiple comparisons from the control (HS Control) there is a statistically significant amount of detectable carbohydrate in both the WB and HS samples. However, the HS sample was more statistically significant as it had a lower P-value. WB control and HS control relationship was not significant (n.s.). The controls were unsonicated samples.

## 4.5 Determining Concentration of *C. neoformans*

To determine the relationship between cell concentration and the amount of capsular PS released from cells in post-sonicated samples of non-melanized *C. neoformans*, H99.

This series of cell concentration experiments were prepared by sonicating non-melanized *C. neoformans*, H99, at  $1 \times 10^6$ ,  $1 \times 10^7$ , and  $1 \times 10^8$  cells/mL then examining the supernatant using a phenol-sulfuric acid assay. Figure 13 shows the result of the phenol-

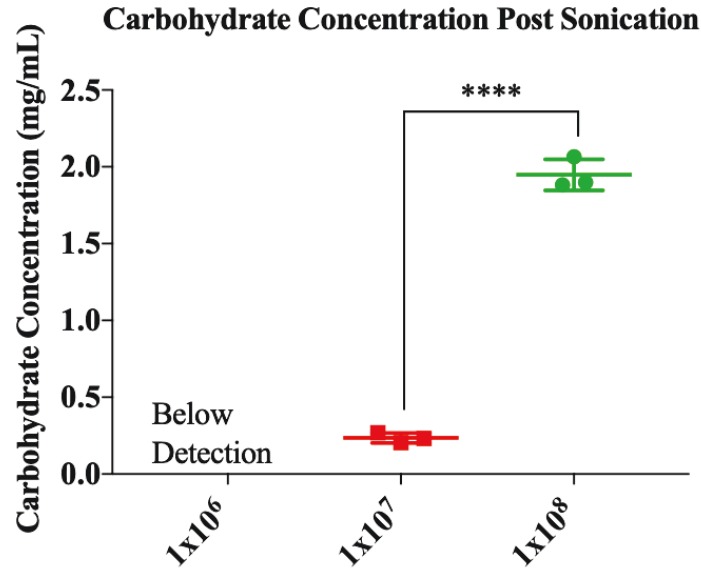


**Figure 13.** Total carbohydrate concentration post-sonication of supernatant samples. Samples of *C. neoformans*, H99, were sonicated at the concentrations noted on the X-axis. The results for  $1 \times 10^6$  cells/mL were below the level of detection. The results for the unsonicated samples were also below the level of detection. This is based on interpolation of a mannose standard curve. The difference between  $1 \times 10^7$  cells/mL and  $1 \times 10^8$  cells/mL was statically significant with a P-value of  $<0.001$  based on an un-paired t test.

sulfuric acid assays that were run on the post-sonicated sample of different densities.

There is statistical significance difference between the  $1 \times 10^7$ , and  $1 \times 10^8$  cells/mL samples. The  $1 \times 10^6$  cells/mL samples were below the level of detection for this assay, thus a carbohydrate concentration could not be determined.

Based on the results from the phenol-sulfuric acid assay (Figure 13), an ELISA to detect GXM in the supernatants of un-sonicated and sonicated samples at different concentrations was run in determine how much GXM was present (Figure 14). I expected to see an increase in GXM as the density of the sonicated samples increased, but instead, the sonicated samples had lower levels of detectable GXM than the high concentration un-sonicated sample (Figure 14).

These unexpected results indicate that GXM, in the form of exo-PS, is being

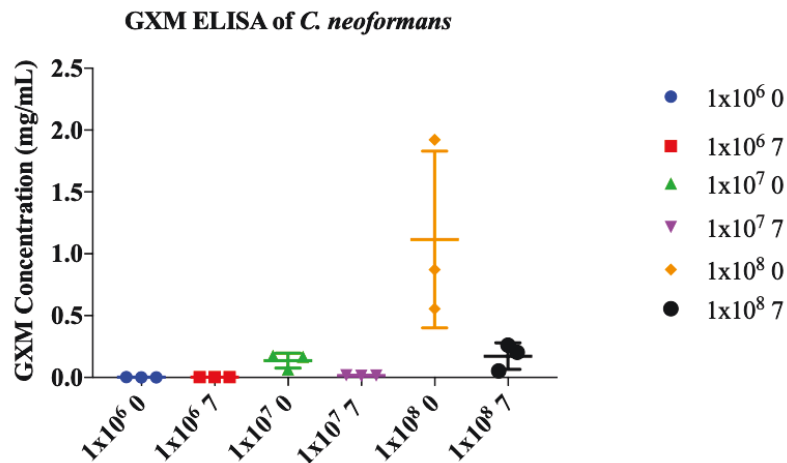


**Figure 14.** GXM concentration of un-sonicated (0) and sonicated (7) samples of *C. neoformans*, H99 at different concentrations (cells/mL). There is a higher amount of detectable GXM in the un-sonicated 1x10<sup>8</sup> cells/mL sample, which could be due to exo-PS being detected. The lack of detectable GXM in the sonicated 1x10<sup>8</sup> cells/mL sample, was surprising and may be due to a change in the GXM epitopes recognized by the primary antibody, 2D10, in this ELISA.

released from the unsonicated 1x10<sup>8</sup> cells/mL sample. It is exo-PS because that is the form of PS that *C. neoformans* is able to shed. This is likely due to the sample sitting dormant while the sonicated samples were being run and the exo-PS not being centrifuged out the sample's supernatant. More interesting, is the lack of detectable GXM in the 1x10<sup>8</sup> cells/mL sonicated sample. There was measurable carbohydrate in these samples (Figure 13) which should indicate GXM within the sample. This lack of

recognition of the GXM antibodies in the ELISA means that the epitopes these antibodies bind to were either not present, or not present in sufficient quantity to allow for binding to occur. It is entirely possible that the GXM epitope for the antibody used in this ELISA, 2D10, is damaged during sonication explaining why it is not able to be detected with this ELISA.

#### **4.6 Sonication of Isolated Exo-PS**

A sample of 100kDa exo-PS, isolated using a 100kDa filter and Amicon filtration, was sonicated using the sonicator level of 7 (approximately 20 Watts (RMS) for 0, 15, 30, 45, and 60 seconds. DLS was then run on these samples to determine the effective diameter (size of the particle determined, by the machine, using the Stokes-Einstein equation<sup>39,52</sup>) of the sample post-sonication. There is a change in the polydispersity of the PS in the samples as they undergo longer lengths of sonication. Polydispersity is a measure of heterogeneity within a sample with higher values corresponding to more size diversity within a sample.

From figure 15, I determined that after 60 seconds of sonication at level 7 the PS was broken into a more polydisperse sample, with a surprisingly high effective diameter. This not only indicates the PS is being cleaved through the use of sonication as the diameter decreases, but that the PS may be aggregating post-sonication. The aggregation is indicated by the larger effective diameter at the 60s time point as noted in figure 15. Aggregation of the PS would mean that the structure is being altered by sonication in a way that promotes subsequent binding together of particulate PS, possibly by exposing new binding sites.

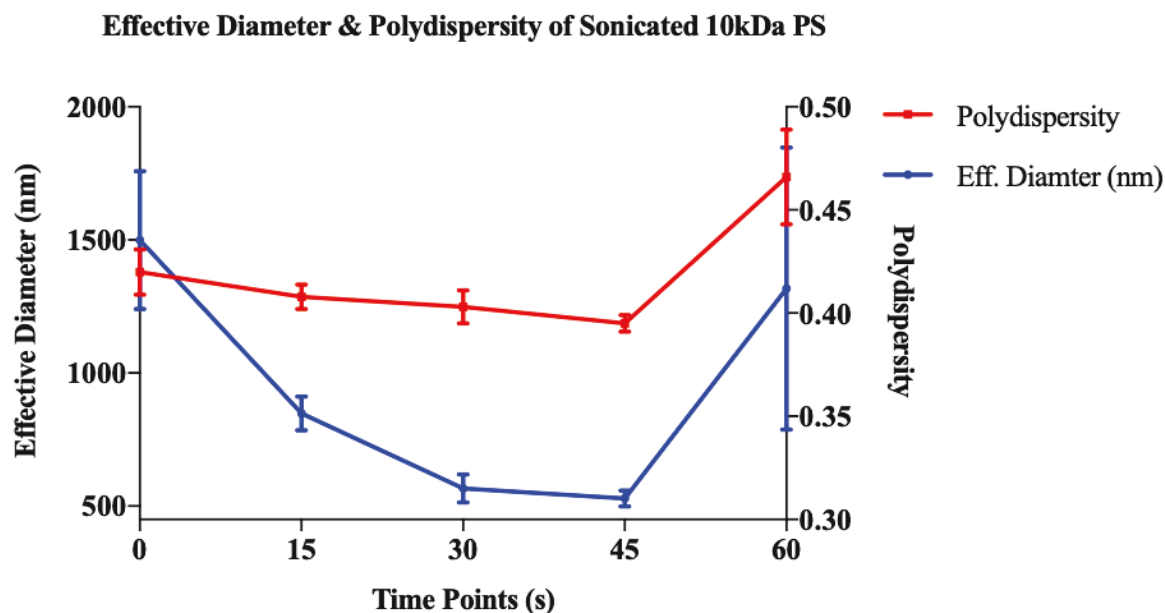


**Figure 15.** Effective diameter and polydispersity of sonicated 10kDa PS from *C. neoformans*  
 As the time increased there the effective diameter decreased indicating the PS was being broken up. The increase at 60s could be due to aggregation of the PS.

#### 4.7 Sonication and Antibody Binding

To further understand what was happening to the PS that remained on the surface of *C. neoformans* post-sonication, I used immunofluorescent microscopy. These results are seen in Table 2. Antibodies to different epitopes on the PS capsule of *C. neoformans* were used to determine if the binding of any of them was affected by sonication.

To determine a change in binding non-melanized *C. neoformans* (un-sonicated, and sonicated) were combined with the following mAbs: 12A1(IgM), 2D10 (IgM), 18B7(IgG1). These are mAbs detect different epitopes within the PS capsule of *C. neoformans* though each binds with a different affinity. 12A1 was also used as it shows whether the binding is annular or punctate within the capsule.<sup>53,54</sup>

From this experiment it was determined that mAb binding to the capsule increased post sonication. This result is exciting because it shows that through sonication the PS capsule of *C. neoformans* is being opened up in such a manner that these mAbs show increased binding to the capsule. This increase was quite remarkable with 12A1. This result may have implications in developing new mAbs for the *C. neoformans* PS capsule.

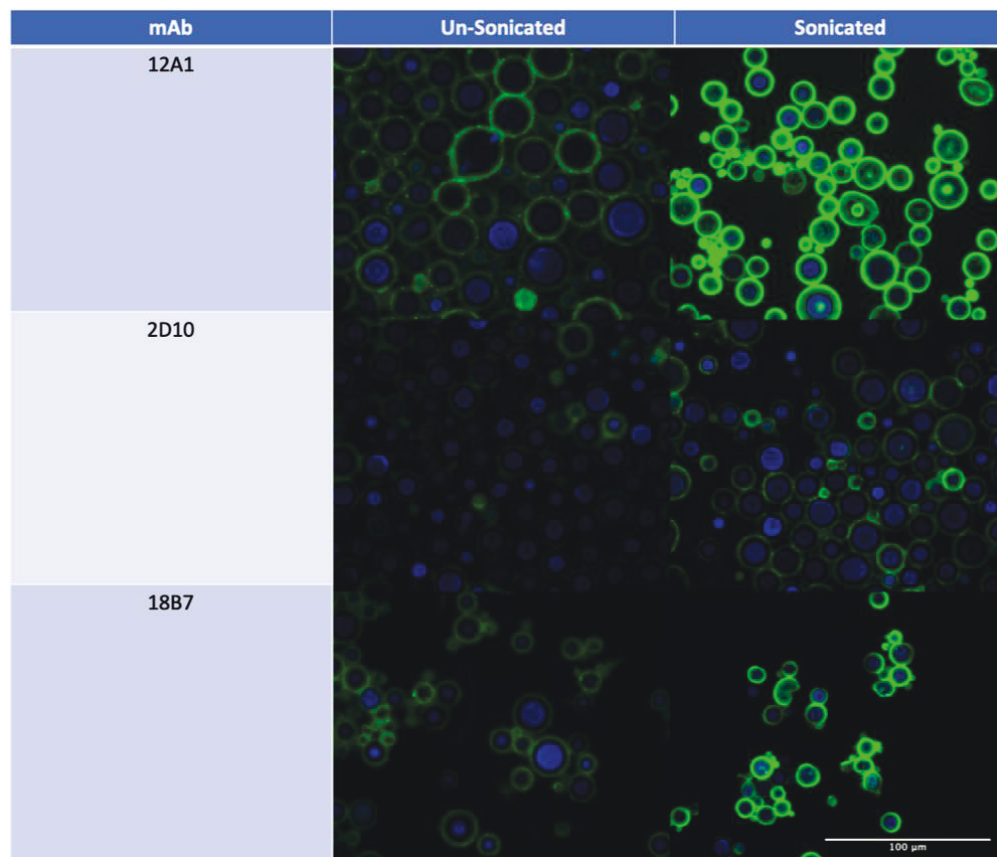


**Table 3.** Immunofluorescent images of un-sonicated and sonicated *C. neoformans* using different mAbs. Post-sonication there is an increase in mAb binding. Images were processed using ImageJ.

## 4.8 Small Angle Neutron Scattering of Exo-PS

Exo-PS with D<sub>2</sub>O and H<sub>2</sub>O, at different concentrations was run on both SANS and

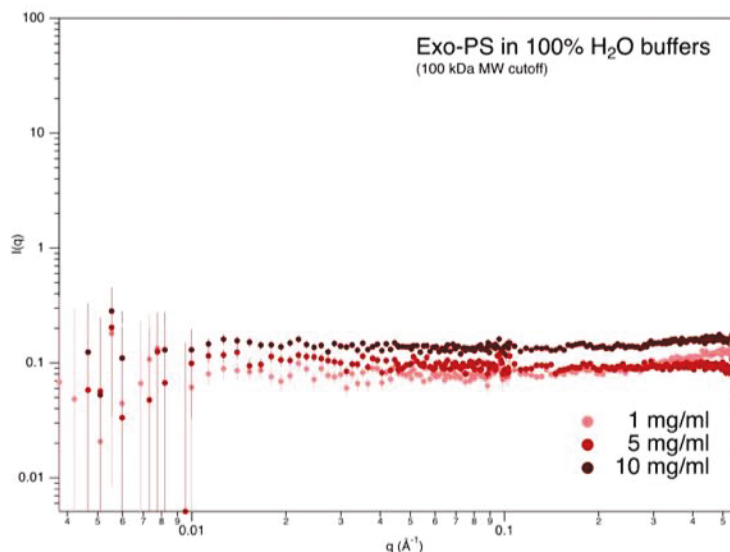


**Figure 16.** Neutron beam scattering readout of *C. neoformans* exo-PS, at different concentrations, in H<sub>2</sub>O on SANS. This was done at different concentrations. The graph is flat which means there are no features in the sample that can be detected. Since it cannot be detected the sample likely has an SLD near H<sub>2</sub>O. Image was created by Dr. Susana Teixeira.

USANS at NIST, with the help of an on-location contact. Exo-PS in H<sub>2</sub>O does not scatter well. It has a scattering light density close to that of H<sub>2</sub>O, which makes it hard to get any readings from either SANS or USANS (*Figure 16*).

For exo-PS samples in D<sub>2</sub>O there was signal on in the SANS regime (*Figure 17*). This is promising because it means we should be able to get structural and composition information from these samples.

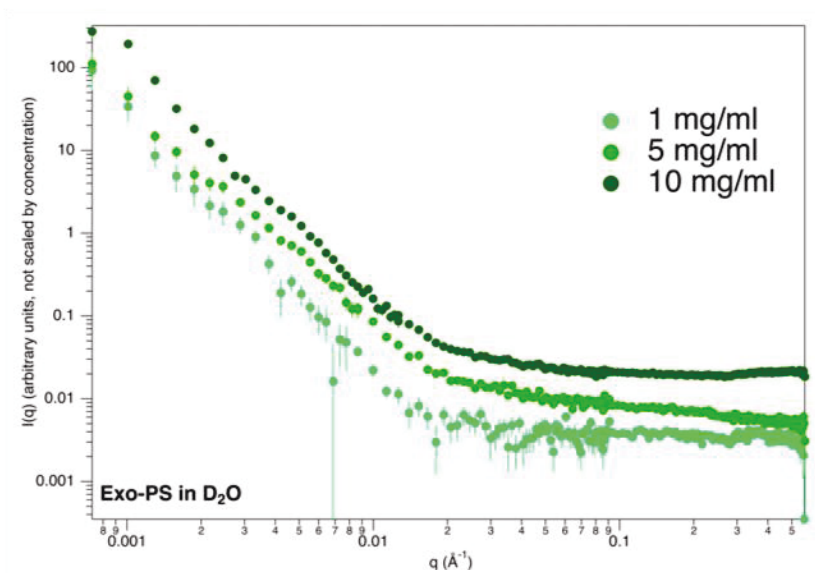


**Figure 17.** Neutron beam scattering readout of *C. neoformans* exo-PS, at different concentrations  $\text{D}_2\text{O}$  on SANS. Signal was detected, Image was created by Dr. Susana Teixeira.



## Discussion

The PS capsule is the main virulence factor for *C. neoformans*. It inhibits phagocytosis by immune cells, interferes with complement, inhibits antibody production, and is necessary to cause disease.<sup>11,13,55</sup> Fragility is the main problem involved when studying capsular components. It is composed of 95% to 99% water with the rest being GXM, GXM-Gal, and mannoproteins.<sup>6</sup> These components form the layered, highly branched, and fragile PS capsule of *C. neoformans*.<sup>4,28</sup> In this study several novel methods, including cavitation induced by ultra-sonication, and probing the exo-PS structure with SANS, and USANS, were used to explore the composition and structure of the PS, exo and capsular, of *C. neoformans*.

This thesis project was initiated to determine if the layer of melanin deposited between the delimiting cell membrane and the polysaccharide (PS) capsule of *C. neoformans* contributes to the physical strength of *C. neoformans* cells when introduced to a physical force. Therefore, I subjected *C. neoformans* cells to multiple different physical stress conditions using cavitation induced by ultra-sonication. I did not see any increased protection in melanized *C. neoformans* when compared to non-melanized. For the initial experiments a water bath sonicator was used to induce cavitation. The water bath sonicator experiments did not reveal any cell breakage, so experiments were moved to the horn sonicator. At first breakage of *C. neoformans* was not seen. Once samples were centrifuged for longer post sonication there was noticeable breakage of cells within the sonicated samples. A noticeable reduction in capsule size post-sonication was seen using a phase contrast microscope using India ink preparations. This indicated that capsules were either lost or compressing. After running multiple tadpoling assays to

determine survival rates, the hypothesis that melanin could help protect *C. neoformans* from sonication was not supported (*Figure 10*). The reduction in capsule size was something that was further explored and became the basis for this thesis.

One interesting finding was that sonication reduced the overall sample (*Figure 7*). The samples were initially the same concentration of cells/mL and despite this, it appears the sonicated samples had fewer cells/mL. This effect could be due to the PS of sonicated cells clumping together or maybe due to the reduction in capsule size post-sonication. The reduction in the PS capsule of *C. neoformans* was seen through the use of India ink imaging (*Figure 8*). India ink is used to see the PS capsule of *C. neoformans* as it provides contrast between the capsule and the background. India ink particles are too large to get into the PS capsule, so the capsule is seen as a halo around the cell body (*Figure 8*).

One explanation about the reduction in the size of the *C. neoformans* capsule was that the capsule was collapsing due to cavitation, this is what I initially thought was happening. This hypothesis was disproven through the use of the phenol-sulfuric acid assay, and the GXM-capture ELISA. If the capsules were collapsing, there should have been no detectable carbohydrate and /or GXM in the supernatant of sonicated samples. This was not the case, however, as there were detectable levels of both in the supernatant of sonicated samples. Based on this evidence it was theorized that cavitation was breaking off parts of the PS capsule and these pieces were released into the supernatant.

For determining the best culture age to perform sonication with *C. neoformans* at 3, 5, and 7 days were sonicated at settings 0-10. From here the supernatant was checked for carbohydrate concentration using a phenol-sulfuric acid assay. The cells were put into

a tadpole assay to determine survival. Based on the results from both of these assays all further experiments were run with culture that was 5 days old and the sonicator was set to 7. *C. neoformans* at higher settings did release more PS into the supernatant and day 7 cultures did have an increase in PS detected as well. The PS capsule is altered with age, which is why a younger culture was decided on despite a lower release in PS. A sonicator level of 7 was chosen because a good quantity of the cells remained alive post sonication.

The use of a water bath sonicator was tested into early in this project as they are standard in most labs and typically used to break up cells. Two samples of *C. neoformans* were prepped and placed in either a water bath for 2 hours or underwent the typically horn sonicator procedure (30 seconds at setting 7). Based on capsule radii measurements it was determined that the water bath did cause a reduction in capsule size. Next, a phenol-sulfuric acid assay was done to determine if the supernatant contained any PS compared to the horn-sonicated sample. There was no detectable PS in the water bath sonicated supernatant. Even when the water bath sonicated supernatant was compared to a sample that had a lower density of *C. neoformans* to begin with. Based on these results experiments using a water bath sonicator did not continue.

To see how much of an effect culture density had on detecting PS in the supernatant has samples containing different densities of *C. neoformans* were sonicated. The densities were  $1 \times 10^6$ ,  $1 \times 10^7$ , and  $1 \times 10^8$  cells/mL. Each of these densities also had a control sample that was not sonicated. The phenol-sulfuric acid assays show that none of the controls or the  $1 \times 10^6$  cells/mL sonicated samples had detectable levels of PS in the supernatant. The sonicated samples with densities of  $1 \times 10^7$ , and  $1 \times 10^8$  cells/mL did have detectable levels.  $1 \times 10^8$  cells/mL samples contained the most detectable PS with a level

of 2.0mg/mL (*Figure 13*) This level was statistically significant compared to  $1 \times 10^7$  cells/mL sonicated sample as determined using an un-paired t test.

Interestingly, the results from the GXM capture ELISA that was run on all the density samples did not detect a large amount of GXM in the supernatant of the sonicated  $1 \times 10^8$  cells/mL samples. This likely means that the PS is being broken up in a way that destroys the epitopes for GXM that 2D10, the primary antibody in the ELISA, bind to. Rather, the highest concentration of GXM was found in the  $1 \times 10^8$  cells/mL un-sonicated samples (*Figure 14*). This could be due to exo-PS being shed into the supernatant during sample preparation, and the samples not being centrifuged enough to get all the PS out of the supernatant. This result supports the idea that sonication is breaking up the PS on the capsule of *C. neoformans*. It also indicates that sonication is changing the epitopes on the capsule. This hypothesis is further supported by the increase in mAb binding activity post sonication (*Table 2*).

Pure 10kDa PS, isolated through filtration from a culture of non-melanized *C. neoformans* was sonicated at different timepoints to determine how the samples would change. Using DLS to obtain polydispersity and effective diameter of the samples (*Figure 15*) there is a decrease in effective diameter, as expected, as time sonicated increases. There is a slight unexpected result in the 60 second timepoint as both the polydispersity and effective diameter of the sample increases. This may be due to some of the PS in the sample beginning to aggregate. The error bars for the 60 second sample are also quite large, so it is not clear if the results for this timepoint are as reliable as the others. As for the other timepoints the error bars are small and show a decrease in effective diameter as the samples are sonicated more. This indicates that the larger PS is

being broken into smaller pieces thus bringing down the average size of the PS. The polydispersity does not change too much from 0-45 seconds, though there is a slight decrease which indicates a slightly more monodisperse sample. This experiment shows that the exo-PS of *C. neoformans* can be broken into smaller pieces using sonication.

Perhaps the most intriguing result obtained from this project is the increased binding of antibodies post sonication (*Table 2*). This is interesting as it may lead to new insights on antibody epitopes on the PS capsule of *C. neoformans*, and virulence may be affected as the immune system may be able to better recognize and bind to the pathogen. The following mAbs were used for this part of the project: 12A1(IgM), 2D10 (IgM), 18B7(IgG1). These are mAbs against the PS capsule of *C. neoformans* though they all bind with different affinities and the epitopes are not fully known. 12A1 in particular bound with much more affinity post sonication. 2D10 and 18B7 did not bind with as high of an affinity as 12A1.

This leads to the question: What is being opened up in the capsule that allows for this increase in mAb binding? One hypothesis is that the epitope for 12A1 is contained on an inner layer (or structural component) of the PS capsule. Disruption of the capsule from sonication allows for this layer to be more exposed than usual, thus the mAb binding is far greater. This may also explain why the other mAbs also bind better post sonication, although it should be noted that the increase was not as great for 2D10, and 18B7.

The work at NIST with SANS and USANS is not complete. What the graphs (*Figure 16*, *Figure 17*) show is simply whether or not it is possible to observe scattering from the neutron beams. With the H<sub>2</sub>O exo-PS samples more work needs to be done in order to get scattering. It may be possible to run the samples on different instruments.

Presently, the concentration of the samples is not high enough to be able to get good neutron beam scattering. There are also problems with the polydispersity of the samples being too high. This means that the sample is too heterogenous, which makes neutron scattering more difficult. The data from the D<sub>2</sub>O samples is also not fully complied. However, for these samples there is scattering. With more modeling work a size and composition should be able to be determined.

## Conclusion

For the component on cavitation our results show that the PS capsule can be removed from *C. neoformans* within 30 seconds. The removed PS can be detected in the supernatant of the sonicated samples through both phenol-sulfuric acid assays, and GXM-capture ELISA. The removal of PS capsule can be seen in India ink images as the cells post sonication have a reduction in capsule radii. There was also shown to be increased levels of binding post-sonication. This suggests that disruption of the capsule is revealing more epitopes for them to bind to on the PS.

Sonication does not add any chemicals to the samples, such as DMSO, that may alter the chemical composition of the PS. This suggests that the PS that is released is in a more natural state then when treated with gamma irradiation or DMSO (*Table 1*). Dehydration of the PS capsule is also not a problem with this method as it keeps the sample in liquid.

More work is needed to acquire data from NIST to determine whether or not scattering occurs. Neutron scattering data could theoretically provide more insight into the structure and composition of the PS of *C. neoformans*. More time needed for computer modeling of samples in order to make any conclusions about this data. Another problem is dealing with a high concentration of exo-PS as it turns into a thick gel making it hard to transfer into the holders that go into the SANS and USANS beams. Diluting the sample has been tried, but there is still not a good signal from either SANS or USANS.

For future work it will be important to determine how this method affects the ability of *C. neoformans* to produce and maintain disease. It is possible that the increased ability of antibodies to bind to the capsule post-sonication would lead the immune system

to be able to clear the infection. The study could then test whether mice who were able to clear the infection were better protected from un-sonicated capsular *C. neoformans*. If the mice were able to better clear an infection from sonicated *C. neoformans* maybe the antibodies produced from this would better protect from further *C. neoformans* infection. Another aspect of this project that could still be explored is to determine how to use sonication, medically, to help clear infections with *C. neoformans*. Since sonication allows for better antibody binding would it may be possible to sonicate infected parts of a patient (mouse or human), and to stimulate their immune system clear the infection. Continuation of this work could also lead to further characterization of the capsule of *C. neoformans* in its natural state—research that is needed to advance the development of a viable vaccine and additional drug targets for *C. neoformans* infections.



## Bibliography

1. C. neoformans Infection Statistics | Fungal Diseases | CDC. Available at: <https://www.cdc.gov/fungal/diseases/ cryptococcosis-neoformans/statistics.html>. Accessed March 22, 2019.
2. Rajasingham R, Smith RM, Park BJ, et al. Global burden of disease of HIV-associated cryptococcal meningitis: an updated analysis. *Lancet Infect. Dis.* 2017;17(8):873-881. doi:10.1016/S1473-3099(17)30243-8.
3. Zaragoza O, Rodrigues ML, De Jesus M, Frases S, Dadachova E, Casadevall A. Chapter 4 The Capsule of the Fungal Pathogen Cryptococcus neoformans. In: Vol 68. *Advances in Applied Microbiology*. Elsevier; 2009:133-216. doi:10.1016/S0065-2164(09)01204-0.
4. Cordero RJB, Frases S, Guimarães AJ, Rivera J, Casadevall A. Evidence for branching in cryptococcal capsular polysaccharides and consequences on its biological activity. *Mol. Microbiol.* 2011;79(4):1101-1117. doi:10.1111/j.1365-2958.2010.07511.x.
5. Casadevall A, Coelho C, Cordero RJB, et al. The Capsule of Cryptococcus neoformans. *Virulence* 2018;0. doi:10.1080/21505594.2018.1431087.
6. Maxson ME, Cook E, Casadevall A, Zaragoza O. The volume and hydration of the Cryptococcus neoformans polysaccharide capsule. *Fungal Genet. Biol.* 2007;44(3):180-186. doi:10.1016/j.fgb.2006.07.010.
7. Buchanan KL, Murphy JW. What makes Cryptococcus neoformans a pathogen? *Emerging Infect. Dis.* 1998;4(1):71-83. doi:10.3201/eid0401.980109.
8. Kozel TR, Cazin J. Nonencapsulated Variant of Cryptococcus neoformans I. Virulence Studies and Characterization of Soluble Polysaccharide. *Infect. Immun.* 1971;3(2):287-294.
9. Currie BP, Casadevall A. Estimation of the prevalence of cryptococcal infection among patients infected with the human immunodeficiency virus in New York City. *Clin. Infect. Dis.* 1994;19(6):1029-1033.
10. Frases S, Pontes B, Nimrichter L, Viana NB, Rodrigues ML, Casadevall A. Capsule of Cryptococcus neoformans grows by enlargement of polysaccharide molecules. *Proc. Natl. Acad. Sci. USA* 2009;106(4):1228-1233. doi:10.1073/pnas.0808995106.
11. Kwon-Chung KJ, Rhodes JC. Encapsulation and melanin formation as indicators of virulence in Cryptococcus neoformans. *Infect. Immun.* 1986;51(1):218-223.
12. Sloan DJ, Parris V. Cryptococcal meningitis: epidemiology and therapeutic options. *Clin Epidemiol* 2014;6:169-182. doi:10.2147/CLEP.S38850.
13. Cordero RJB, Pontes B, Guimarães AJ, et al. Chronological aging is associated with biophysical and chemical changes in the capsule of Cryptococcus neoformans. *Infect. Immun.* 2011;79(12):4990-5000. doi:10.1128/IAI.05789-11.
14. Cherniak R, Sundstrom JB. Polysaccharide antigens of the capsule of Cryptococcus neoformans. *Infect. Immun.* 1994;62(5):1507-1512.
15. Wang Y, Aisen P, Casadevall A. Cryptococcus neoformans melanin and virulence: mechanism of action. *Infect. Immun.* 1995;63(8):3131-3136.
16. Alp S. [Melanin and its role on the virulence of Cryptococcus neoformans].

- Mikrobiyol Bul* 2010;44(3):519-526.
17. Jacobson ES, Tinnell SB. Antioxidant function of fungal melanin. *J. Bacteriol.* 1993;175(21):7102-7104.
  18. Casadevall A, Rosas AL, Nosanchuk JD. Melanin and virulence in *Cryptococcus neoformans*. *Curr. Opin. Microbiol.* 2000;3(4):354-358. doi:10.1016/S1369-5274(00)00103-X.
  19. Henson JM, Butler MJ, Day AW. THE DARK SIDE OF THE MYCELIUM: melanins of phytopathogenic fungi. *Annu. Rev. Phytopathol.* 1999;37:447-471. doi:10.1146/annurev.phyto.37.1.447.
  20. Eisenman HC, Nosanchuk JD, Webber JBW, Emerson RJ, Camesano TA, Casadevall A. Microstructure of cell wall-associated melanin in the human pathogenic fungus *Cryptococcus neoformans*. *Biochemistry* 2005;44(10):3683-3693. doi:10.1021/bi047731m.
  21. d'Ischia M, Wakamatsu K, Napolitano A, et al. Melanins and melanogenesis: methods, standards, protocols. *Pigment Cell Melanoma Res* 2013;26(5):616-633. doi:10.1111/pcmr.12121.
  22. Nicolaus RA, Piattelli M, Fattorusso E. The structure of melanins and melanogenesis—IV. *Tetrahedron* 1964;20(5):1163-1172. doi:10.1016/S0040-4020(01)98983-5.
  23. Riley PA. Melanin. *Int. J. Biochem. Cell Biol.* 1997;29(11):1235-1239. doi:10.1016/S1357-2725(97)00013-7.
  24. Melanin | C<sub>18</sub>H<sub>10</sub>N<sub>2</sub>O<sub>4</sub> - PubChem. Available at: <https://pubchem.ncbi.nlm.nih.gov/compound/Melanin>. Accessed April 12, 2019.
  25. Williamson PR. Biochemical and molecular characterization of the diphenol oxidase of *Cryptococcus neoformans*: identification as a laccase. *J. Bacteriol.* 1994;176(3):656-664.
  26. Berzelius JJ. *Lehrbuch Der Chemie.*; 1840:522.
  27. Cleare W, Casadevall A. Scanning electron microscopy of encapsulated and non-encapsulated *Cryptococcus neoformans* and the effect of glucose on capsular polysaccharide release. *Med Mycol* 1999;37(4):235-243.
  28. Maxson ME, Dadachova E, Casadevall A, Zaragoza O. Radial mass density, charge, and epitope distribution in the *Cryptococcus neoformans* capsule. *Eukaryotic Cell* 2007;6(1):95-109. doi:10.1128/EC.00306-06.
  29. Cherniak R, Reiss E, Turner SH. A galactoxylomannan antigen of *Cryptococcus neoformans* serotype A. *Carbohydr. Res.* 1982;103(2):239-250. doi:10.1016/S0008-6215(00)80686-2.
  30. Bloomfield N, Gordon MA, Elmendorf DF. Detection of *cryptococcus neoformans* antigen in body fluids by latex particle agglutination. *Proc Soc Exp Biol Med* 1963;114:64-67.
  31. Diamond RD. Prognostic factors in cryptococcal meningitis. *Ann. Intern. Med.* 1974;80(2):176. doi:10.7326/0003-4819-80-2-176.
  32. Cherniak R, Valafar H, Morris LC, Valafar F. *Cryptococcus neoformans* chemotyping by quantitative analysis of <sup>1</sup>H nuclear magnetic resonance spectra of glucuronoxylomannans with a computer-simulated artificial neural network. *Clin Diagn Lab Immunol* 1998;5(2):146-159.
  33. Belay T, Cherniak R. Determination of antigen binding specificities of

- Cryptococcus neoformans factor sera by enzyme-linked immunosorbent assay. *Infect. Immun.* 1995;63(5):1810-1819.
34. Frases S, Nimrichter L, Viana NB, Nakouzi A, Casadevall A. Cryptococcus neoformans capsular polysaccharide and exopolysaccharide fractions manifest physical, chemical, and antigenic differences. *Eukaryotic Cell* 2008;7(2):319-327. doi:10.1128/EC.00378-07.
  35. De Jesus M, Nicola AM, Rodrigues ML, Janbon G, Casadevall A. Capsular localization of the Cryptococcus neoformans polysaccharide component galactoxylomannan. *Eukaryotic Cell* 2009;8(1):96-103. doi:10.1128/EC.00331-08.
  36. Vaishnav VV, Bacon BE, O'Neill M, Cherniak R. Structural characterization of the galactoxylomannan of Cryptococcus neoformans Cap67. *Carbohydr. Res.* 1998;306(1-2):315-330. doi:10.1016/S0008-6215(97)10058-1.
  37. Overview of Mass Spectrometry | Thermo Fisher Scientific - US. Available at: <https://www.thermofisher.com/us/en/home/life-science/protein-biology/protein-biology-learning-center/protein-biology-resource-library/pierce-protein-methods/overview-mass-spectrometry.html>. Accessed February 20, 2019.
  38. McFadden DC, Fries BC, Wang F, Casadevall A. Capsule structural heterogeneity and antigenic variation in Cryptococcus neoformans. *Eukaryotic Cell* 2007;6(8):1464-1473. doi:10.1128/EC.00162-07.
  39. Some D. Light-scattering-based analysis of biomolecular interactions. *Biophys. Rev.* 2013;5(2):147-158. doi:10.1007/s12551-013-0107-1.
  40. Goren MB, Middlebrook GM. Protein conjugates of polysaccharide from Cryptococcus neoformans. *J. Immunol.* 1967;98(5):901-913.
  41. Dembitzer HM, Buza I, Reiss F. Biological and electron microscopic changes in gamma radiated Cryptococcus neoformans. *Mycopathol Mycol Appl* 1972;47(3):307-315.
  42. Bryan RA, Zaragoza O, Zhang T, Ortiz G, Casadevall A, Dadachova E. Radiological studies reveal radial differences in the architecture of the polysaccharide capsule of Cryptococcus neoformans. *Eukaryotic Cell* 2005;4(2):465-475. doi:10.1128/EC.4.2.465-475.2005.
  43. Brennen CE. Cavitation in medicine. *Interface Focus* 2015;5(5):20150022. doi:10.1098/rsfs.2015.0022.
  44. Brennen CE. *Cavitation and Bubble Dynamics*. Cambridge: Cambridge University Press; 2013. doi:10.1017/CBO9781107338760.
  45. Barker JG, Glinka CJ, Moyer JJ, Kim MH, Drews AR, Agamalian M. Design and performance of a thermal-neutron double-crystal diffractometer for USANS at NIST. *J Appl Crystallogr* 2005;38(6):1004-1011. doi:10.1107/S0021889805032103.
  46. Instrument - BT5 USANS - Ultra Small Angle Neutron Scattering. Available at: <https://www.ncnr.nist.gov/equipment/msnew/ncnr/bt5-usans-ultra-small-angle-neutron-scattering.html>. Accessed February 13, 2019.
  47. Kline SR. Reduction and analysis of SANS and USANS data using IGOR Pro. *J Appl Crystallogr* 2006;39(6):895-900. doi:10.1107/S0021889806035059.
  48. Glinka CJ, Barker JG, Hammouda B, Krueger S, Moyer JJ, Orts WJ. The 30 m Small-Angle Neutron Scattering Instruments at the National Institute of Standards and Technology. *J Appl Crystallogr* 1998;31(3):430-445.

doi:10.1107/S0021889897017020.

49. Welch AZ, Koshland DE. A simple colony-formation assay in liquid medium, termed 'tadpoling', provides a sensitive measure of *Saccharomyces cerevisiae* culture viability. *Yeast* 2013;30(12):501-509. doi:10.1002/yea.2989.
50. Casadevall A, Mukherjee J, Scharff MD. Monoclonal antibody based ELISAs for cryptococcal polysaccharide. *J. Immunol. Methods* 1992;154(1):27-35. doi:10.1016/0022-1759(92)90209-C.
51. Masuko T, Minami A, Iwasaki N, Majima T, Nishimura S-I, Lee YC. Carbohydrate analysis by a phenol-sulfuric acid method in microplate format. *Anal. Biochem.* 2005;339(1):69-72. doi:10.1016/j.ab.2004.12.001.
52. Stetefeld J, McKenna SA, Patel TR. Dynamic light scattering: a practical guide and applications in biomedical sciences. *Biophys. Rev.* 2016;8(4):409-427. doi:10.1007/s12551-016-0218-6.
53. Nussbaum G, Cleare W, Casadevall A, Scharff MD, Valadon P. Epitope location in the *Cryptococcus neoformans* capsule is a determinant of antibody efficacy. *J. Exp. Med.* 1997;185(4):685-694.
54. Cleare W, Casadevall A. The different binding patterns of two immunoglobulin M monoclonal antibodies to *Cryptococcus neoformans* serotype A and D strains correlate with serotype classification and differences in functional assays. *Clin Diagn Lab Immunol* 1998;5(2):125-129.
55. Bulmer GS, Tacker JR. Phagocytosis of *Cryptococcus neoformans* by alveolar macrophages. *Infect. Immun.* 1975;11(1):73-79.

## Camilla A. Strother

510 S. Ann St. • Baltimore, MD 21231 • Phone: 857-222-6479 • E-Mail: cstroth2@jhu.edu

### Education

Johns Hopkins Bloomberg School of Public Health August 2017-May 2019  
Master of Science, Molecular Microbiology and Immunology

Johns Hopkins Bloomberg School of Public Health August 2017-May 2018

Certificate in Vaccine Science and Policy

University of Massachusetts, Amherst September 2012 – May 2016  
BS, Microbiology  
BA, History

### Experience

Master of Science Research Student, Johns Hopkins Bloomberg School of Public Health  
August 2017-May 2019

- Develop and execute experiments for my master's thesis and publication
- Present my research at weekly lab meetings and provide input on lab mate's presentations
- Present research findings at departmental forums
- Order materials for the lab and maintain an organized, detailed lab notebook
- Train new lab members and people from other labs on use of various equipment

Bacteriology Services Technician, Animal Diagnostic Laboratory, Penn State University February 2017-June 2017

- Conducted diagnostic testing using a variety of bacteriology and molecular microbiology techniques
- Performed sample setup, bacterial enumeration, and identification
- Maintained laboratory sections including weekly laboratory inventory

Teaching Assistant, Introductory Microbiology Lab for Majors, UMass, Amherst  
September 2015-May 2016

- Assisted 20+ undergraduate microbiology majors with basic microbiology lab techniques in a BSL-2 level laboratory class
- Organized materials for each lab, explained lab procedures and experiment results, assisted students in use of bright field and phase contrast microscopy, incubated all media inoculated during a lab period, supervised students to ensure lab safety procedures were followed, and assisted students in writing up lab discussions
- Instructed students on the work for the day before class
- Graded laboratory notebooks, and helped students organize their laboratory reports

EMT-Basic, UMass Amherst Emergency Medical Service September 2014  
– May 2016

- Monitored patrons at campus events and provided basic life support as needed

Teaching Assistant, EMT-Basic Course, UMass, Amherst September 2014 –  
September 2015

- Taught students the practical techniques needed to pass the national and MA state EMS exam, including upper and lower back splinting, CPR, back boarding, seated extrication, and handling a range of medical emergency scenarios
- Graded student exams, and their ability to perform practical skills like splints

Emergency Room Volunteer, Cooley Dickinson Hospital May 2015 –  
August 2015

- Aided medical staff in cleaning and preparing rooms new patients
- Prepared meals and snacks for patients

- Kept the patients up to date with where their tests were

Emergency Room Volunteer, Beth-Israel Deaconess Plymouth  
August 2014

May 2014 –

- Delivered medical samples from the emergency room to the diagnostic laboratory
- Kept the waiting room clean and organized
- Cleaned patient rooms and areas once they were vacant

### **Laboratory and Related Skills**

- |  |                                      |
|--|--------------------------------------|
| • R Studio                             | • Flow cytometry                     |
| • Igor64                               | • Spectrophotometer reading analysis |
| • Data collection and analysis         | • Microscopy                         |
| • Immunofluorescence assay             | • Microbiological techniques         |
| • Antibody isolation and purification  | • PCR                                |
| • Testing antibody purification        | • Fungal Culture                     |
| • GXM- Capture ELISA                   | • Polysaccharide Isolation           |
| • Size exchange chromatography         | • Phenol-Sulfuric Acid Assay         |
| • Ion exchange chromatography          | • Sonication of cells                |
| • Gram staining                        | • Tadpoling                          |
| • Streak plating for isolated colonies | • Melanin Isolation                  |
| • Identification of unknown bacteria   |                                      |
| • SDS-PAGE                             |                                      |

### **Trainings/Certificates**

- National Institute of Standards and Technology Laboratory and Radiation Training
- Bloodborne Pathogens
- Good Clinical Practice Certificate
- Title IX Certificate

### **References**

#### **Arturo Casadevall, MD, PhD.**

Chair, Molecular Microbiology & Immunology  
Johns Hopkins Bloomberg School of Public Health  
615 N. Wolfe Street  
Baltimore, Maryland 21205  
410-955-3457  
[acasadevall@jhu.edu](mailto:acasadevall@jhu.edu)

#### **Radamés J.B. Cordero, Ph.D.**

Research Associate, Molecular Microbiology & Immunology  
Johns Hopkins Bloomberg School of Public Health  
615 N. Wolfe Street  
Baltimore, Maryland 21205  
[rcorder4@jhu.edu](mailto:rcorder4@jhu.edu)

#### **Gundula Bosch, Ph.D.**

Program Director for R3, Assistant Scientist, Molecular Microbiology & Immunology  
Johns Hopkins Bloomberg School of Public Health  
615 N. Wolfe Street  
Baltimore, Maryland 21205  
[gbosch2@jhu.edu](mailto:gbosch2@jhu.edu)